

Spin Splitting of Landau Levels and the Effective g Factor in Gray Tin*

B. L. BOOTH† AND A. W. EWALD

Northwestern University, Evanston, Illinois 60201

(Received 26 May 1969)

Spin splitting of magnetoresistance oscillations was observed in Sb-doped gray-tin samples having a low electron concentration ($8 \times 10^{15} \text{ cm}^{-3}$) and also in those in a high-concentration range (10^{18} – 10^{19} cm^{-3}). The high-concentration samples showed splitting for both longitudinal and transverse magnetic-field configurations; in low-concentration samples the high-field-component peaks disappeared as the field was rotated from a transverse to a longitudinal direction. The splitting factor Δ_s ($2\Delta_s/\hbar\omega$ equals the Landau-level splitting) was evaluated for the field in principal crystallographic planes. The angular dependence of Δ_s is similar to that of the oscillatory period, reflecting the shape of the Fermi surface. Values of the effective spectroscopic splitting factor $|g|$ evaluated from the Δ_s values for various field directions and electron concentrations ranged between 7.5 and 27.5.

I. INTRODUCTION

IN addition to the orbital quantization of electron energies into Landau levels, a magnetic field lifts the degeneracy of electron spin states, thereby splitting the original Landau levels. Necessary conditions for the resolution of spin-split Landau levels at moderate field strengths are (i) a small effective mass and (ii) a large absolute value of the effective g factor. From $\mathbf{k} \cdot \mathbf{p}$ perturbation theory, a low effective mass and a high g value are direct consequences of a low value of the pertinent interacting energy gap.¹ Work of several investigators has shown that in InSb the conditions for resolved spin splitting are adequately met^{2–5}; the electron effective mass is $0.016m_e$ and the g factor is about -50 . The latter value has been determined experimentally by oscillatory magnetoresistance^{3,4} and magneto-optical absorption⁵ and has also been calculated theoretically.⁵ In Ge it has been shown that the g factor is near -3.7 in $\langle 100 \rangle$ directions and -2.3 in $\langle 111 \rangle$ directions,⁵ values which compare well with the theoretical predictions of Cohen and Blount.⁶ The g factor of conduction electrons differs from the free-electron value of 2 because of spin-orbit coupling, and its magnitude can greatly exceed 2 if there is a three-fold orbital degeneracy or if the spin-orbit splitting becomes large compared with the pertinent interacting energy gap.⁶ Both of the above are true or nearly so for most elemental and zinc-blende-type semiconductors.⁷

* Research supported by the Advanced Research Projects Agency of the Department of Defense through the Northwestern Materials Research Center and by the National Science Foundation. The work is part of a dissertation submitted by one of the authors (B.L.B.) to the Graduate School of Northwestern University in partial fulfillment of the requirements for the Ph.D. degree.

† Present address: E. I. du Pont de Nemours & Co., Engineering Physics Laboratory, Wilmington, Del.

¹ C. Kittel, *Quantum Theory of Solids* (John Wiley & Sons, Inc., New York, 1963), Chap. 14.

² H. P. R. Frederikse and W. R. Hosler, *Phys. Rev.* **108**, 1136 (1957).

³ R. A. Isaacson and M. Weger, *Bull. Am. Phys. Soc.* **9**, 736 (1964).

⁴ G. A. Antcliffe and R. A. Stradling, *Phys. Letters* **20**, 119 (1966).

⁵ L. M. Roth, B. Lax, and S. Zwerdling, *Phys. Rev.* **114**, 90 (1959).

⁶ M. H. Cohen and E. I. Blount, *Phil. Mag.* **5**, 115 (1960).

In the course of investigating the symmetry,⁸ non-parabolicity,⁹ and ionized-impurity scattering¹⁰ of the Γ -centered conduction electrons in Sb-doped gray tin by oscillatory magnetoresistance, we observed spin-split oscillations in samples for which the ionized-impurity scattering was weak. Sufficiently weak scattering occurred in the lightly doped samples ($N_d \approx 8 \times 10^{15} \text{ cm}^{-3}$) because of the low concentration of scattering centers, and also in samples for which $10^{18} \leq N_d \leq 10^{19} \text{ cm}^{-3}$ because of the very effective screening of ionized impurities by the high-mass electrons in the L -centered states which begin to be populated at a donor concentration of $5 \times 10^{17} \text{ cm}^{-3}$.

We expect the effective g factor for gray tin to lie between the above values for Ge and InSb because the interacting gap $E_G = 0.41 \text{ eV}$ ¹¹ lies between those of Ge (0.89 eV) and InSb (0.23 eV). Furthermore, the higher bands which determine the nonsphericity of the Γ_8^+ conduction and valence bands are expected to affect the g factor in a similar fashion.¹² Consequently, the spin splitting should have an angular dependence similar to that recently published for the gray-tin conduction-band Fermi surface.⁸

In this paper we present and discuss the data on the angular dependence and the donor-concentration dependence of spin splitting of Landau levels in gray tin. From the data, we obtain the corresponding dependences of the g factor. The apparatus and experimental procedure as well as the methods of crystal growth, selection, and orientation have been described previously.^{8,9}

II. THEORY

In a sufficiently high magnetic field, electrons occupy one-dimensional harmonic-oscillator states with respect

⁷ J. Callaway, *Energy Band Theory* (Academic Press Inc., New York, 1964), Sec. 3.5.

⁸ B. L. Booth and A. W. Ewald, *Phys. Rev.* **168**, 805 (1968).

⁹ B. L. Booth and A. W. Ewald, *Phys. Rev.* **168**, 796 (1968).

¹⁰ B. L. Booth and A. W. Ewald, *Phys. Rev. Letters* **18**, 491 (1967).

¹¹ S. H. Groves, C. R. Pidgeon, R. J. Wagner, and A. W. Ewald, *Bull. Am. Phys. Soc.* **13**, 429 (1968).

¹² S. H. Groves, R. N. Brown, and C. R. Pidgeon, *Phys. Rev.* **161**, 779 (1967).

to their motion perpendicular to the field, while motion parallel to the field is unaffected by quantization. The degeneracy of the electron spin states is also lifted. Consequently, the electron energy for a free-electron-like system with the magnetic field in the z direction is the sum of these three contributions:

$$E = (n + \frac{1}{2})\hbar\omega + \hbar^2 k_z^2 / 2m_z^* \pm \beta_0 g \frac{1}{2} B, \quad (1)$$

where $\omega = eB/m^*c$ is the cyclotron frequency which depends on the cyclotron effective mass m^* . $\beta_0 = eh/2m_e c$ is the Bohr magneton, B is the magnetic field, g is the effective spectroscopic splitting factor, and k_z and m_z^* are the z components of the wave vector and effective-mass tensor, respectively. Here n is the Landau-level number which takes on positive-integer values including zero. With increasing field, the Landau-level spacing $\hbar\omega$ increases so that the levels appear to approach and pass through the Fermi surface. This produces fluctuations in the density of states at the Fermi surface which are periodic in reciprocal field and which are manifest as fluctuations or oscillations in the electronic properties.

The periodicity in reciprocal field can be seen in the free-electron-like case by rewriting Eq. (1) for level number n at the Fermi surface:

$$E_F = (n + \frac{1}{2} \pm \Delta_s)\hbar\omega, \quad (2)$$

where $\Delta_s \equiv gm^*/4m_e \equiv \frac{1}{4}gm'$. Rearranging, we have

$$1/B = (n + \frac{1}{2} \pm \Delta_s)eh/m^*cE_F, \quad (3)$$

or that the period $P \equiv \Delta(1/B) = eh/m^*cE_F$, since successive Landau levels are located at the Fermi surface when n changes by 1. In a real crystal the effective mass may not be the same at all points of the electron orbit. In this case the cross-sectional area between Landau levels is still quantized and the area \mathcal{Q} corresponding to level n is given by¹³

$$\mathcal{Q} = (n + \frac{1}{2} \pm \Delta_s)2\pi eB/ch \quad (4)$$

or

$$1/B = (n + \frac{1}{2} \pm \Delta_s)2\pi e/ch\mathcal{Q}. \quad (5)$$

Both Eqs. (3) and (5) may be expressed as

$$n = 1/BP - \frac{1}{2} \pm \Delta_s. \quad (6)$$

Thus, plotting Landau-level numbers against the reciprocals of the field values of the split magnetoresistance peaks yields two straight lines separated vertically by $2\Delta_s$, the level splitting in units of $\hbar\omega$.

A relation similar to Eq. (6) is obtained from the theory of transverse magnetoresistance given by Adams and Holstein¹⁴ when this theory is appropriately modified to include spin splitting.⁶ The previously published⁹ expression for the oscillatory component of magnetoresistance under the conditions of our experi-

¹³ J. M. Ziman, *Electrons and Phonons* (Oxford University Press, London, 1962), pp. 513–523.

¹⁴ E. N. Adams and T. D. Holstein, *J. Phys. Chem. Solids* **10**, 254 (1959).

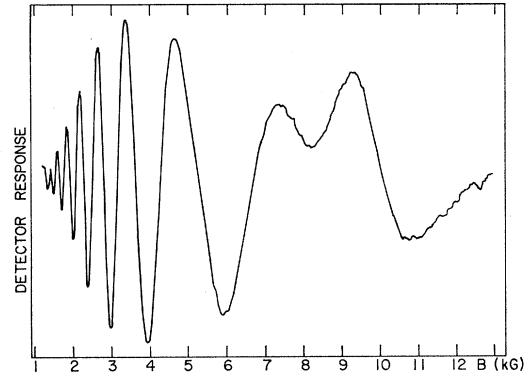


FIG. 1. Magnetoresistance oscillations for a sample with $N_d = 7.6 \times 10^{15} \text{ cm}^{-3}$ at $T = 1.35^\circ\text{K}$ with the magnetic field in a $\langle 100 \rangle$ direction transverse to the current. Spin splitting of the $n=1$ Landau level produces the well-resolved component peaks at 7.4 and 9.25 kG.

ments is

$$\Delta\rho/\rho_0 = -A \cos(2\pi/PB - \frac{1}{4}\pi) \cos\frac{1}{2}\pi m'g, \quad (7)$$

where

$$A = C \left[-J_2(\alpha) \right] \frac{(T + T_i) e^{-\beta T_D m'/B}}{B^{1/2} \sinh[\beta(T + T_i)m'/B]} \quad (8)$$

and $C = 5\sqrt{2}\pi^2 k_B (m^*c/E_F eh)^{1/2}$, a constant for a particular sample and field orientation. $J_2(\alpha)$ is the Bessel function of order 2 and argument $\alpha = 2\pi B_m/PB^2$, where B_m is the amplitude of the modulated field; $\beta = 2\pi k_B \times m_e c/eh$; T_D is the Dingle temperature which measures the broadening of Landau levels due to scattering by ionized impurities; and T_i is the empirically introduced inhomogeneity temperature which measures the level broadening due to sample inhomogeneity.⁹

In connection with the amplitude expression, it may be noted that the observation of magnetoresistance oscillations requires some appropriate combination of small effective mass, low sample and effective temperatures, and high magnetic field. Another requirement is that of statistical degeneracy. These conditions are conveniently summarized in the statement⁹

$$E_F > \hbar\omega > k_B(T + T_D + T_i) \equiv k_B T'. \quad (9)$$

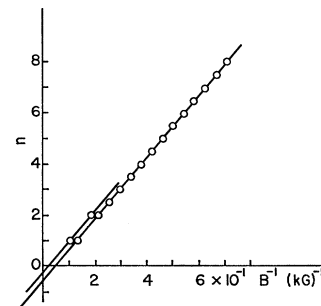


FIG. 2. Integer-versus- $1/B$ plot for the oscillations of Fig. 1.

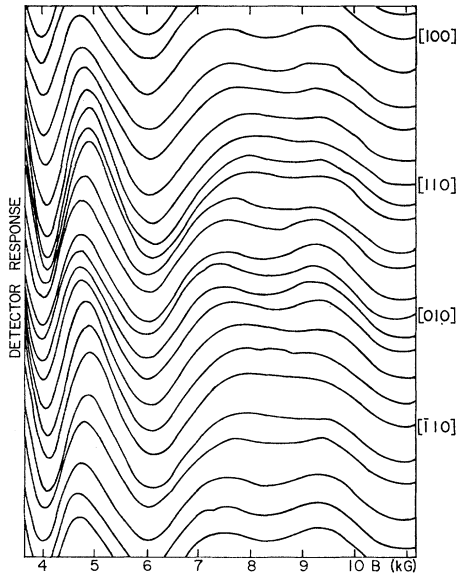


FIG. 3. Spin splitting of the $n=1$ Landau level for various field directions in a $\{100\}$ plane. Other conditions are the same as for the trace of Fig. 1. The systematic variation in the location of the unsplit peak near 5 kG is due to the slight nonsphericity of the Fermi surface.

Resolution of spin splitting imposes the further requirement that $2\Delta_s\hbar\omega$ be greater than $k_B T'$.

Considering now Eq. (7), the minus sign may be absorbed by introducing $-\pi$ in the argument of the first cosine function and, using a trigonometric identity, we have

$$\Delta\rho/\rho_0 = \frac{1}{2}A \left[\cos 2\pi \left(\frac{1}{PB} - \frac{5}{8} - \Delta_s \right) + \cos 2\pi \left(\frac{1}{PB} - \frac{5}{8} + \Delta_s \right) \right]. \quad (10)$$

Again plotting integers against the $1/B$ values of the oscillation peaks (which correspond to the dc maxima),¹⁵ we have two straight lines given by

$$n = 1/PB - \frac{5}{8} \pm \Delta_s. \quad (11)$$

TABLE I. Values of the spin-splitting factor Δ_s and the effective spectroscopic splitting factor, $|g|$ for principal directions and various Sb donor concentrations. ($2\Delta_s\hbar\omega$ equals the Landau-level splitting.)

N_d (cm^{-3})	$\langle 100 \rangle$		$\langle 110 \rangle$		$\langle 111 \rangle$	
	Δ_s	$ g $	Δ_s	$ g $	Δ_s	$ g $
7.6×10^{15}	0.164 ± 0.007	27.5 ± 1.0	0.129 ± 0.007	20.7 ± 1.0	0.12 ± 0.01	18.5 ± 1.5
1.0×10^{18}	0.150 ± 0.005	18.8 ± 1.0
2.5×10^{18}	0.150 ± 0.005	17.0 ± 1.0	0.105 ± 0.01	11.0 ± 1.5	0.075 ± 0.015	7.5 ± 1.5
5.0×10^{18}	0.150 ± 0.005	16.2 ± 1.0

¹⁵ S. S. Shalym and A. L. Efros, Fiz. Tverd. Tela **5**, 1233 (1962) [English transl.: Soviet Phys.—Solid State **4**, 903 (1962)].

This expression differs from Eq. (6) only in the numerical phase factor.

In practice, Δ_s and φ are evaluated more precisely by the following procedure: For a particular split Landau level n , the high-energy component passes through the Fermi surface first with increasing field, and consequently has the lower field value B_+ . Similarly, B_- locates the low-energy or high-field peak. Therefore, from Eqs. (6) or (11), letting φ equal the numerical phase factor, we have

$$n = 1/PB_+ - \varphi - \Delta_s = 1/PB_- - \varphi + \Delta_s \quad (12)$$

or

$$\Delta_s = (1/2P)(1/B_+ - 1/B_-). \quad (13)$$

To evaluate φ , Eq. (11) may be written

$$1/P = (n + \varphi - \Delta_s)B_- = (n + \varphi + \Delta_s)B_+ \quad (14)$$

or

$$n + \varphi = \Delta_s(B_- + B_+) / (B_- - B_+). \quad (15)$$

III. DATA ANALYSIS AND RESULTS

The conditions of our experiments were such that the Dingle temperature was the dominant factor determining whether or not spin splitting could be observed.^{9,10} The inhomogeneity temperatures of the samples selected for study fell in the range 0.25–2.7°K. With a minimum sample temperature of 1.3°K, Eq. (9) imposes an upper limit of a few degrees on T_D , and this was confirmed by the observations. The dependence of T_D on the (ionized) donor concentration N_d is the following.^{10,16}

Starting at 2°K at $N_d \cong 8 \times 10^{15} \text{ cm}^{-3}$, it rises as $N_d^{1/3}$ to a value of 10°K at $N_d \cong 5 \times 10^{17} \text{ cm}^{-3}$. Then, with the onset of screening by the L_6^+ electrons, it drops sharply to an essentially constant value of 1°K for $10^{18} \leq N_d \leq 10^{19} \text{ cm}^{-3}$. Thus, observation of spin splitting is confined to a low-concentration range extending up to about $8 \times 10^{15} \text{ cm}^{-3}$ and the high-concentration range between 10^{18} and 10^{19} cm^{-3} . We will treat the two ranges separately.

An example of the spin splitting in a low-concentration sample ($N_d = 7.6 \times 10^{15} \text{ cm}^{-3}$) is shown in Fig. 1.

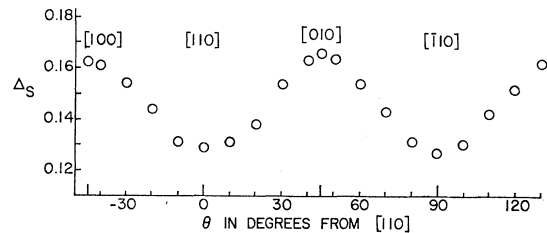


FIG. 4. Spin-splitting parameter Δ_s versus field orientation in a $\{100\}$ plane for the sample of Fig. 1.

¹⁶ B. L. Booth, Ph.D. thesis, Northwestern University, 1967 (unpublished).

¹⁷ R. H. Traxler, Bull. Am. Phys. Soc. **9**, 736 (1964).

¹⁸ G. Dresselhaus, A. F. Kip, and C. Kittel, Phys. Rev. **98**, 368 (1955).

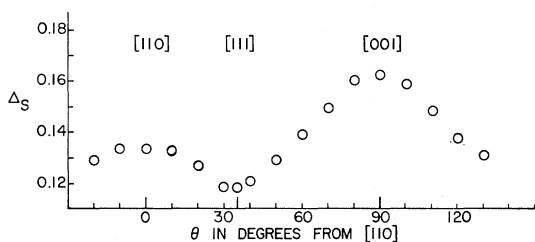


FIG. 5. Spin-splitting parameter Δ_s versus field orientation in a $\{110\}$ plane for the sample of Fig. 1.

It shows the oscillations at 1.35°K for the field in a $\langle 100 \rangle$ direction transverse to the current. The well-resolved component peaks at 7.4 and 9.25 kG are identified with the $n=1$ Landau level through the integer-versus- $1/B$ plot of Fig. 2. (Splitting of the $n=2$ peak was evidenced in the original trace by a barely discernible shoulder on the main peak.) Substitution into Eq. (13) of the above field values together with $P=8.23 \times 10^{-5} \text{ G}^{-1}$ (evaluated from the slope in Fig. 2) yields $\Delta_s=0.166$. The phase factor φ is then found to be -0.48 from Eq. (15). Similar analyses of the data for other principal directions yielded the Δ_s values given in Table I. Also tabulated are the g values calculated from Δ_s and the previously published effective masses.⁹

The variation of the splitting as the transverse field was rotated in a principal plane was also investigated. The traces for the (001) plane are shown in Fig. 3. Except for the varying field direction and a lower amplifier gain, the experimental conditions were the same as for the trace of Fig. 1. Analysis [using Eq. (13)] of these and similar data for the (110) plane yielded the angular dependences of Δ_s shown in Figs. 4 and 5.

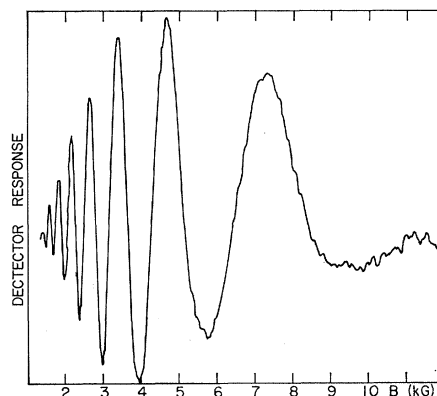


FIG. 6. Oscillations under the same conditions as for Fig. 1 except that the field is parallel to the current. The high-field component of the spin-split peak disappears as the field is rotated from the transverse to the longitudinal direction.

The symmetry displayed here is the same as that of the angular dependence of the oscillatory period.⁸

A qualitatively different spin-splitting behavior is observed in the longitudinal magnetoresistance of these low-concentration samples. The trace of Fig. 6 was

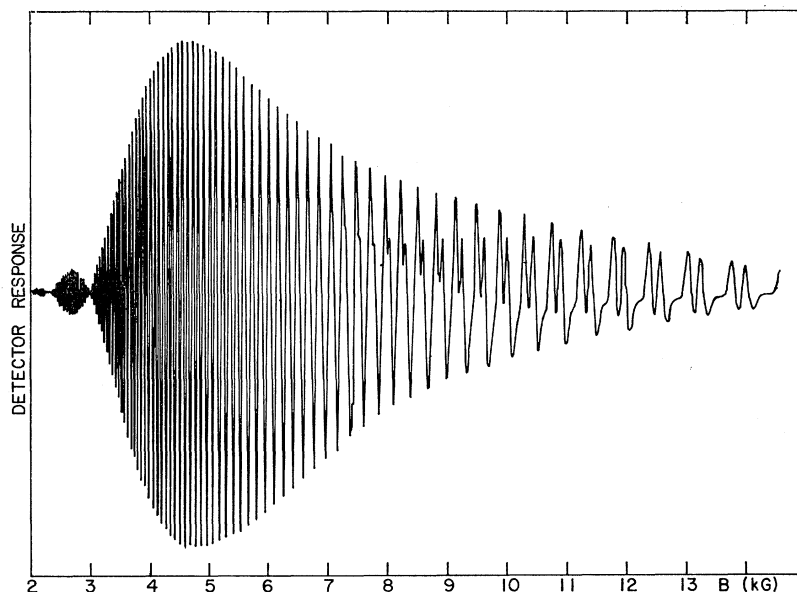
TABLE II. Comparison of mass energy gap E_g , spin-orbit splitting Δ , the $k=0$ conduction-band-edge reduced mass m' , and the effective g factor for Ge, α -Sn, and InSb.

	E_g (eV)	Δ (eV)	m'	$ g $
Ge	0.89	0.3	0.041	3.0
α -Sn	0.41 ^a	0.80 ^a	0.0236	22.2 ^b
InSb	0.24	0.9	0.016	50.0

^a S. H. Groves, C. R. Pidgeon, R. J. Wagner, and A. W. Ewald, Bull. Am. Phys. Soc. 13, 429 (1968).

^b Average of low-electron-concentration values.

FIG. 7. Oscillations for a high-electron-concentration sample ($N_d=2.5 \times 10^{18} \text{ cm}^{-3}$) at $T=1.33^\circ\text{K}$ with the magnetic field in a $\langle 100 \rangle$ direction transverse to the current. Nodes at low magnetic fields and constriction of the high-field amplitude are due to field modulation.



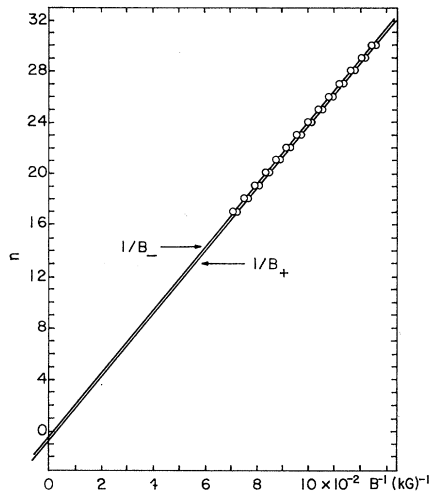


FIG. 8. Integer-versus- $1/B$ plot for oscillations of Fig. 7.

obtained under conditions the same as for Fig. 1, except that here both the current and field were in a $\langle 100 \rangle$ direction. Clearly, the high-field component of the $n=1$ split peak has vanished. Upon rotating from the transverse to the longitudinal direction, the component peaks do not coalesce; the high-field component just disappears. Apart from the $n=1$ and $n=2$ peaks, the oscillations for the two geometries are identical. This behavior has been observed by others in InSb^{2-4} and some attempt has been made to explain it by postulating different scattering rates for spin-up and spin-down electrons.^{4,17}

Turning now to the high-concentration region, the first indication of spin splitting is observed at $N_d=7 \times 10^{17} \text{ cm}^{-3}$. At this concentration a slight shoulder appears on the high-field oscillations. When $N_d=2.5 \times 10^{18} \text{ cm}^{-3}$, the Dingle temperature has reached its lowest value and spin splitting is well resolved.

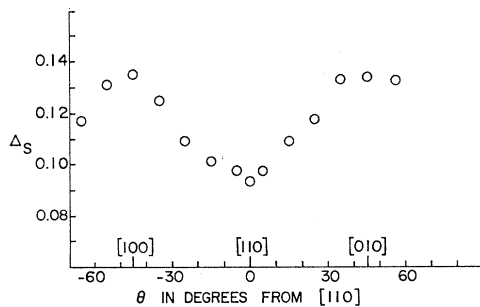


FIG. 9. Spin-splitting parameter Δ_s versus field orientation in a $\{100\}$ plane for the sample of Fig. 7.

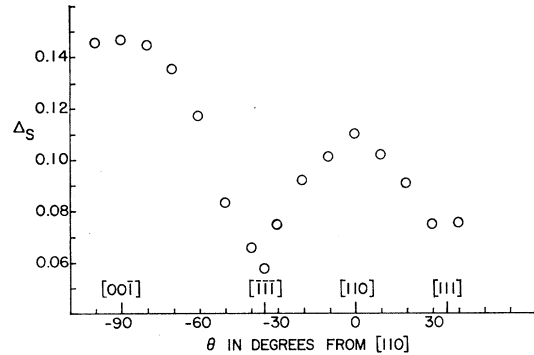


FIG. 10. Spin-splitting parameter Δ_s versus field orientation in a $\{110\}$ plane for the sample of Fig. 7.

Figure 7 shows data at 1.33°K for this concentration with the transverse field in a $\langle 100 \rangle$ direction. The distortion of the high-field oscillation valleys is not angular-dependent and is attributed to higher harmonic content. The integer-versus- $1/B$ values of the component peaks are plotted in Fig. 8. The intercept again gives $\varphi \cong -\frac{1}{2}$. Traces similar to that of Fig. 7 were recorded for various field directions in the (001) and $(1\bar{1}0)$ planes. The Δ_s values deduced from the several split peaks of a given trace were averaged and these average values are plotted against field direction in Figs. 9 and 10. The angular dependence is the same as for the low-concentration samples, and similar to that found in Ge.⁵ An interesting but unexplained difference between the two concentration regions is the persistence in the high-concentration case of both spin-split-component peaks as the field is rotated to the longitudinal direction.

Table I summarizes the principal-direction results obtained for all samples showing resolved spin splitting. The g factor reflects the concentration-dependent mass or nonparabolicity of the band. Table II shows the systematic variation of the g values and related band parameters for Ge, $\alpha\text{-Sn}$, and InSb . The higher-lying Γ_{15} conduction band is primarily responsible for the nonsphericity of the Fermi surface in Ge¹⁸ and $\alpha\text{-Sn}$.⁸ The observed similarity between the anisotropy of Δ_s and the oscillatory period⁸ supports the recent suggestion¹² that the spin-splitting anisotropy is also determined by Γ_{15} .

A further study of the spin splitting of Landau levels in gray tin by means of the magnetoresistance oscillations is planned. In particular, samples having donor concentrations less than $8 \times 10^{15} \text{ cm}^{-3}$ will be investigated in an effort to observe the splitting of the $n=0$ Landau level and its dependence on field direction.